JOTCS A
Journal of the Turkish Chemical Society
Section: A
Chemistry
TURKISH CHEMICAL SOCIETY

Hydrothermal Syntheses, Crystal Structures, and Properties of 1D Coordination Polymers Based on 5-Nitroisophthalic Acid and 1-Methylimidazole Linkers

Mürsel Arıcı[1]*

[1]Eskişehir Osmangazi University, Faculty of Science and Arts, Department of Chemistry, 26480, Eskişehir, Turkey.

Abstract: Two new coordination polymers, namely $[Mn(\mu_3\text{-}5\text{-nip})(1\text{-meim})_2(H_2O)]_n$ (**1**) and $\{[Co(\mu\text{-}5\text{-nip})(1\text{-meim})_3]\cdot H_2O\}_n$ (**2**) (5-nip: 5-nitroisophthalate, 1-meim: 1-methylimidazole), were hydrothermally synthesized and characterized by FTIR spectroscopy, elemental analysis, single crystal X-ray diffraction, and simultaneous thermal analysis techniques. The 5-nip ligand exhibited two different coordination modes in its structures. In **1** and **2**, 1D chains were generated by 5-nip ligands and metal(II) ions. In **1** and **2**, 5-nip ligand coordinated to three Mn(II) and two Co(II) ions as bis(monodentate) bridging mode and a monodentate and bidentate chelating modes, respectively. For **1** and **2**, 2D supramolecular layers were formed by hydrogen bonds which were extend into 3D supramolecular structures via π···π stacking interactions between two symmetry–related imidazole rings of neighboring molecules. Furthermore, optical and thermal properties of the complexes were also studied.

Keywords: 5-nitroisophthalate, coordination polymer, optical properties.

Submitted: September 25, 2017. **Accepted:** March 29, 2018.

Cite this: Arıcı M. Hydrothermal Syntheses, Crystal Structures, and Properties of 1D Coordination Polymers Based on 5-Nitroisophthalic Acid and 1-Methylimidazole Linkers. JOTCSA. 2018;5(2):653–64.

DOI: http://dx.doi.org/10.18596/jotcsa.339915.

***Corresponding author.** E-mail: marici@ogu.edu.tr, Tel: +902222393750, Fax: +902222393578).

INTRODUCTION

In recent years, the field of crystal engineering of coordination polymers has received considerable interest due to their interesting architectures and their application areas such as gas adsorption/separation, magnetism, sensor, luminescence, and catalysis, *etc*. (1-6). For the above-mentioned applications, the selections of organic building blocks and metal ions are crucial factors in the construction of coordination polymers with desired architecture (7, 8). Moreover, several factors as *e.g.* metal-ligand ratio, temperature, and pH have influence on the final structure (9). In the synthesis of coordination polymers, aromatic multi-carboxylic acids, especially dicarboxylic acid as an anionic ligand have been extensively preferred owing to their diverse coordination modes and structural stabilities in their complexes (10). Hence, in this study, 5-nitroisophthalic acid was selected as an anionic ligand in the construction of coordination polymers. It can connect to metal ions with four potential oxygen donor atoms from two carboxylate groups with the bending angle of 120° and its 5-substituted nitro group has electron withdrawing ability and steric effect (11-14) (Scheme 1). Moreover, mixed-ligand coordination polymers (with dicarboxylic acid and N- donor neutral ligand) have been widely synthesized to improve the structural diversity and dimensionality in the assembly process (7, 15). 1-methylimidazole ligand was used as a secondary neutral ligand to provide geometric need of metal centers. In this work, two 1D mixed-ligand Mn(II) and Co(II) coordination polymers, $[Mn(\mu_3\text{-}5\text{-nip})(1\text{-meim})_2(H_2O)]_n$ (**1**) and $\{[Co(\mu\text{-}5\text{-nip})(1\text{-meim})_3]\cdot H_2O\}_n$ (**2**) were hydrothermally synthesized with 5-nipH_2 and 1-meim ligands and characterized by using FTIR spectroscopy, single crystal X-ray diffraction, elemental analysis, and thermal analysis techniques (TG/DTA). Moreover, diffuse reflectance spectra of the compounds were recorded and band-gaps of the complexes were calculated by using Kubelka-Munk function (16).

EXPERIMENTAL SECTION

Materials and measurements

All reagents were of analytical grade and used without further purification. Perkin-Elmer 2400C elemental analyzer was used for elemental analyses (CHN). FTIR spectra using KBr pellets were acquired with a Bruker Tensor 27 spectrometer device in the range of 4000–400 cm^{-1}. The diffuse reflectance spectra (DRS) were obtained with Shimadzu UV-2600 spectrophotometer using $BaSO_4$ as a reference in the wavelength range 200–800 nm. TG/DTA analyses were measured on a Perkin Elmer Diamond TG/DTA Thermal Analyzer from 30 to 700 °C under static air. A Bruker Smart Apex II CCD with a D8-QUEST diffractometer equipped with a graphite-monochromatic Mo-Kα radiation (λ = 0.71073 Å) was used for single crystal data collections at 296 K. The structure solutions and refinements were performed with direct methods using SHELXT and full-matrix least-squares on all F^2 data using SHELXL in connection with the OLEX2 software (17). Refinements of all non-hydrogen atoms were carried out with anisotropic

parameters. Molecular graphics were drawn with Mercury software (18). Crystallographic information files are deposited with the CCDC 1576332 and 1576333.

Syntheses

[Mn(μ$_3$-5-nip)(1-meim)$_2$(H$_2$O)]$_n$ (**1**)*:* $Mn(CH_3COO)_2{\cdot}4H_2O$ (1 mmol, 0.245 g) and 5–nitroisophthalic acid (5-nipH_2) (1 mmol, 0.22 g) were mixed in water (20 mL) and stirred at 70 ^oC for an hour and then 1- methylimidazole (1-meim) (3 mmol, 0.246 g) was added into the mixture. The final mixture was placed in a 25 mL closed capped-glass bottle and heated at 120 ^oC for four days to obtain colorless crystals of **1**. (Yield: 0.112 g, 25.11 % based on $Mn(CH_3COO)_2{\cdot}4H_2O$). Anal. Calcd. for $C_{16}H_{17}MnN_5O_7$: C, 43.06; H, 3.84; N, 15.69 %. Found: C, 43.56; H, 3.38; N, 15.13 %. FTIR (KBr, cm^{-1}): 3356, 3288, 3129, 3316, 3089, 2967, 1629, 1612, 1562, 1535, 1453, 1373, 1346, 1106, 942, 840, 762, 738 cm^{-1}.

{[Co(μ-5-nip)(1-meim)$_3$]·H$_2$O}$_n$ (**2**)*:* The procedure for preparation of complex **2** was similar to that used for **1**, except that the $Co(CH_3COO)_2{\cdot}4H_2O$ (1 mmol, 0.249 g) was used instead of $Mn(CH_3COO)_2{\cdot}4H_2O$. After hydrothermal conditions, the resulting mixture was filtered and evaporated at room temperature. The purple-colored crystals of **2** were obtained (Yield: 0.168 g, 31.58% based on $Co(CH_3COO)_2{\cdot}4H_2O$). Anal. Calcd. for $C_{20}H_{23}CoN_7O_7$: C, 45.12; H, 4.35; N, 18.42 %. Found: C, 44.97; H, 4.41; N, 18.02 %. FTIR (KBr, cm^{-1}): 3509, 3373, 3146, 3112, 3051, 2963, 1629, 1615, 1564, 1534, 1368, 1344, 1104, 944, 840, 731 cm^{-1}.

Scheme 1: Coordination modes of 5-nip ligand in its compounds

RESULTS AND DISCUSSION

Synthesis and characterization

The complexes were hydrothermally synthesized by using $M(CH_3COO)_2{\cdot}4H_2O$ (M: Mn(II) and Co(II)), 5-nipH_2 and 1-meim ligands. The complexes were characterized with various techniques. In the FTIR spectra of the complexes, the broad bands appearing in the range of 3556-3509 cm^{-1} are assigned to v(O–H) stretching vibrations of coordinated and uncoordinated water molecules. For **1** and **2**, the bands observed between 3146 and 3051 cm^{-1} are due to aromatic v(C–H) stretchings. For **1** and **2**, aliphatic v(C–H) stretching vibrations of 1-meim ligand appeared at 2967 and 2963 cm^{-1}, respectively. For both complexes, the bands observing between at 1629 and 1612 cm^{-1} and between at 1373 and 1368 cm^{-1} are due to the asymmetric (ν_{asym}(COO)) and symmetric (ν_{sym}(COO)) stretching vibrations of 5-nip, respectively.

Description of crystal structure

Table 1 indicates the crystal data and structural refinement parameters.

Table 1: Crystal data and structural refinement parameters for **1** and **2.**

	1	**2**
Empirical formula	$C_{16}H_{17}MnN_5O_7$	$C_{20}H_{23}CoN_7O_7$
Formula weight	446.28	532.38
Crystal system	Triclinic	Monoclinic
Space group	*P*-1	*C*2/c
***a* (Å)**	8.836	20.570
***b* (Å)**	10.162	16.679
***c* (Å)**	11.960	15.327
α(°)	105.12	90
β (°)	105.87	115.99
γ(°)	105.30	90
***V* (Å^3)**	930	4726.8
Z	2	8
***D*$_c$ (g cm^{-3})**	1.594	1.496
μ (mm^{-1})	0.76	0.78
Measured refls.	44930	58988
Independent refls.	4621	5796
***R*$_{int}$**	0.046	0.042
S	1.18	1.21
R1/wR2	0.043/0.110	0.057/0.123
$\Delta\rho_{max}/\Delta\rho_{min}$ (eÅ^{-3})	0.42/−0.78	0.61/−0.55

***[Mn(μ$_3$-5-nip)(1-meim)$_2$(H$_2$O)]$_n$* (1).** The crystal structure of **1** is given in Figure 1 and selected bond distances, angles and hydrogen bond geometries are given in Table 2. X-ray result shows that **1** crystallizes in triclinic system and P-1 space group. The asymmetric unit has one Mn(II) ion, one 5-nip, two 1-meim ligands, and a coordinated water molecule. As seen in Figure 1, each Mn(II) ion is coordinated by three oxygen atoms from different 5-nip ligands, two nitrogen atoms from two different 1-meim ligands, and one oxygen atom from one aqua ligand to form a distorted octahedral geometry. Each nip ligand acts as a μ_3- bridging ligand to connect three Mn(II) ions. Two Mn(II) ions are bridged by two carboxylate groups from two different 5-nip ligands with Mn···Mn distance of 5.017 Å to generate $[Mn_2(CO_2)_2]$ secondary building unit (SBU). SBUs are linked by carboxylate oxygen atoms (O9) of 5-nip to generate 1D chain with 16–membered rings (Figure 2). 1D chains are extend to 2D supramolecular layer with hydrogen bonds between carboxylate oxygen atom ($O4^{ii}$) of 5-nip and coordinated water molecule (O7) and [O7···$O4^{ii}$ = 2.964 Å; O7-H7···$O4^{ii}$ = 155.31°] (ii: 1-x, -y, 1-z) (Figure 3). Moreover, adjacent 2D layers are further connected by π···π stacking interactions between two symmetry–related

imidazole rings of neighboring molecules forming a 3D supramolecular network (Cg1···Cg1^{iii} = 3.719 Å, Cg1: N1-C9-N2-C11-C10, iii: 2-x, 2-y, 2-z) (Figure 3).

Table 2: Selected bond distances (Å), angles (º) and hydrogen-bond geometry data for **1***.

Bond Lengths (Å)				
Mn1–O2^{i}	2.1656 (1)		Mn1–N3	2.2292 (2)
Mn1–O1	2.1649 (1)		Mn1–N1	2.2271 (2)
Mn1–O7	2.2985 (1)		Mn1–O3^{ii}	2.1947 (1)
Angles (º)				
O2^{i}–Mn1–O3^{ii}	93.74 (5)		O1–Mn1–O2^{i}	94.36 (5)
O2^{i}–Mn1–N3	90.50 (6)		O1–Mn1–O7	91.31 (5)
O2^{i}–Mn1–N1	89.30 (6)		N3–Mn1–O7	91.57 (6)
O1–Mn1–N1	93.07 (6)		N1–Mn1–O7	88.33 (6)
O3^{ii}–Mn1–O7	80.63 (5)		N1–Mn1–N3	176.98 (6)
O3^{ii}–Mn1–N3	89.11 (6)		O2^{i}–Mn1–O7	173.97 (5)
Hydrogen bond geometry (Å, °)				
D–H···*A*	*D*–H	H···*A*	*D*···*A*	*D*–H···*A*
O7–H7*B*···O4^{ii}	0.88	1.85	2.722(2)	167 (3)
O7–H7*A*···O4^{iv}	0.80	2.22	2.964(2)	155 (3)

*Symmetry codes: (i) −*x*+1, −*y*+1, −*z*+2; (ii) *x*, *y*+1, *z*; (iii) *x*, *y*−1, *z*, (iv) −*x*+1, −*y*, −*z*+1.

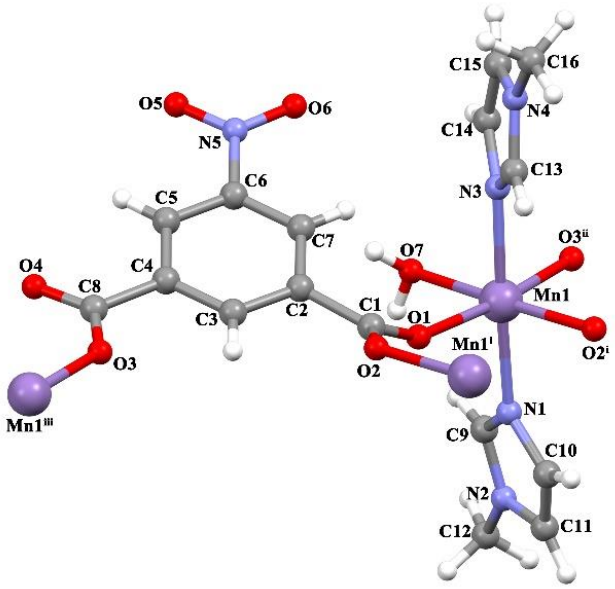

Figure 1: The molecular structure of **1**

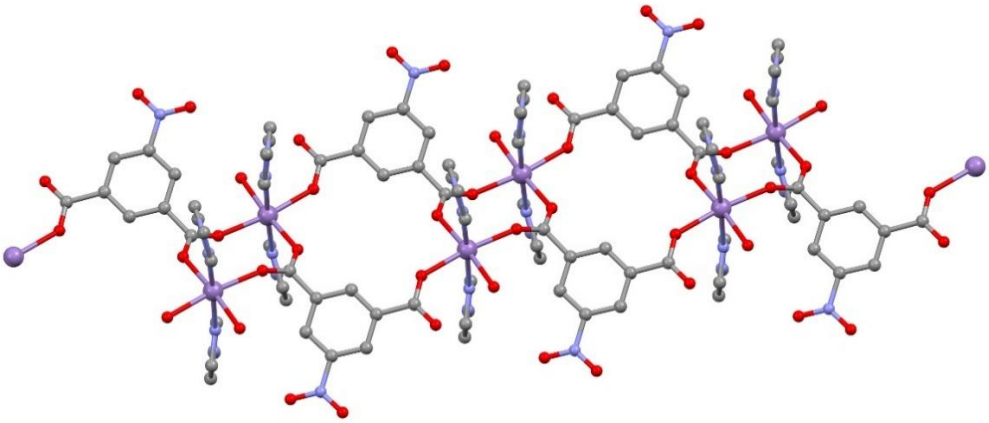

Figure 2: 1D chain structure of complex **1.**

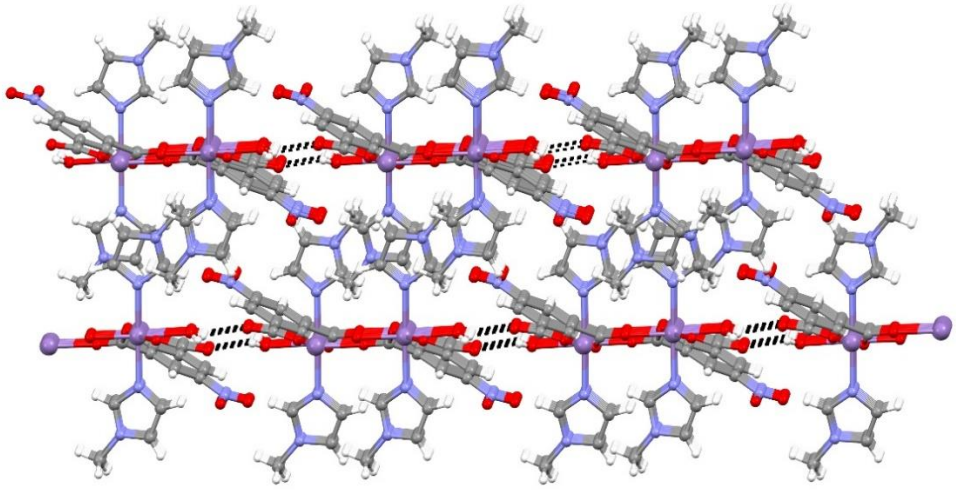

Figure 3: 3D supramolecular structure of complex **1** generated by hydrogen bonds and π···π stacking interactions.

{[Co(μ-5-nip)(1-meim)$_3$]·H$_2$O}$_n$ (2). Table 3 shows the selected bond distances and angles. X-ray result demonstrates that complex **2** crystallizes in monoclinic *C2/c* space group. There are one Co(II) ion, one 5-nip, three 1-meim ligands, and one uncoordinated water molecule in the asymmetric unit (Figure 4). Each Co(II) ion is six-coordinated by three carboxylate oxygen atoms from two different 5-nip ligands and three nitrogen atoms from three different 1-meim ligands.

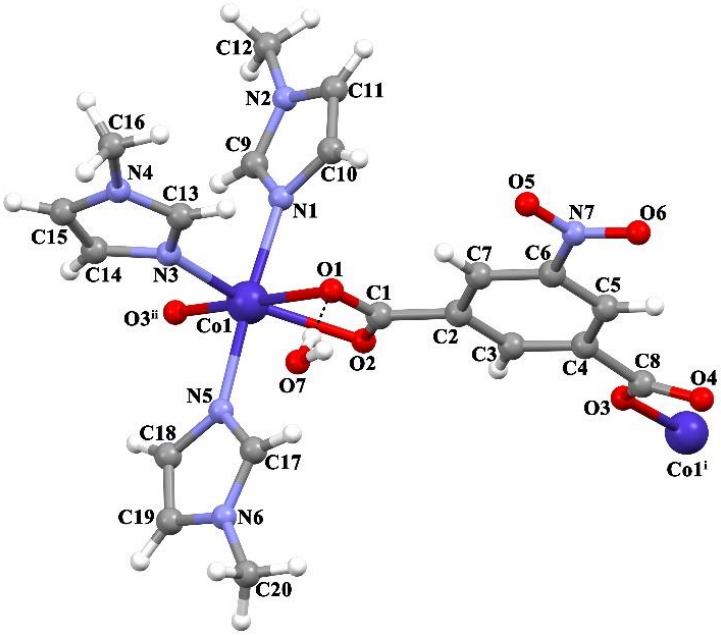

Figure 4: The molecular structure of **2**

In **2**, 5-nip ligand coordinates to two Co(II) ions in monodentate and bidentate chelating modes to form 1D zig-zag chain (Figure 5).

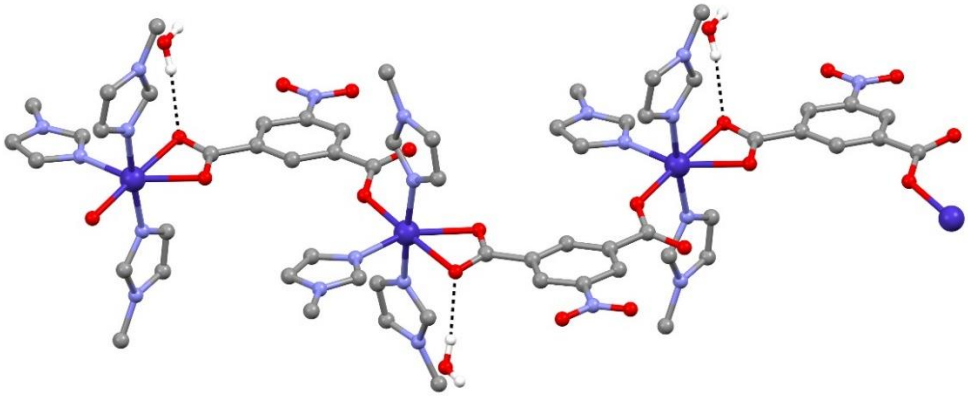

Figure 5: 1D chain structure of complex **2.**

Adjacent 1D chains expand into 2D supramolecular layer with hydrogen bonding between carboxylate oxygen atom (O2) of 5-nip and uncoordinated water molecule (O7) [O2···O7 = 2.76 Å, O2···H7B-O7 = 176.16°] and between uncoordinated carboxylate oxygen atom ($O4^{iii}$) of adjacent 5-nip ligand and water molecule (O7) [O7···$O4^{iii}$ = 2.931 Å, O7-H7A···$O4^{iii}$ = 168.27°] (Figure 6a). Furthermore, 2D layers are further connected by π···π stacking interactions between two symmetry–related imidazole rings of neighboring molecules forming a 3D supramolecular network ($Cg3···Cg3^{iv}$ = 3.719 Å, Cg1: N1-C9-N2-C11-C10, iv: 1/2-x, 1/2-y, 1-z) (Figure 6b).

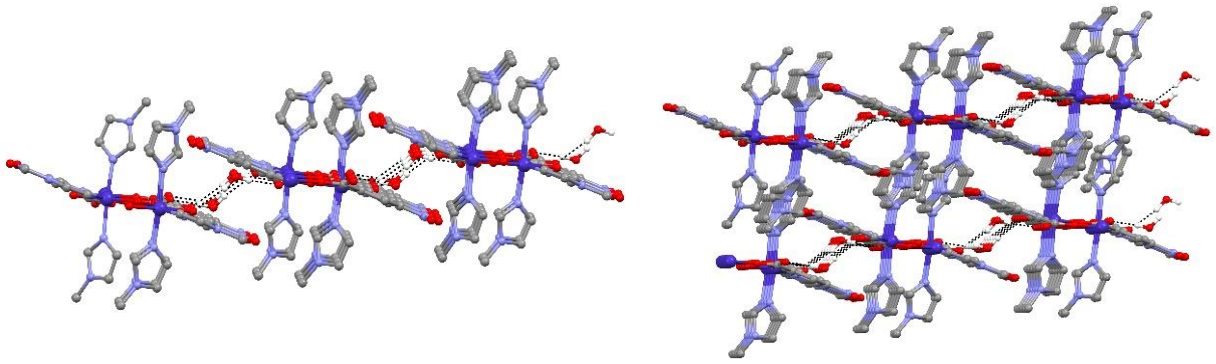

(a) **(b)**

Figure 6: (a) 2D supramolecular layer of complex **2** generated by hydrogen bondings **(b)** 3D supramolecular structure of complex **2** generated by π···π stacking interactions

Table 3: Selected bond distances (Å), angles (º) and hydrogen-bond geometry data for **2***.

Bond Lengths (Å)				
Co1–O4^{i}	2.293 (2)	Co1–N1		2.115 (2)
Co1–O3^{i}	2.241 (2)	Co1–N5		2.122 (2)
Co1–O1	2.0714 (2)	Co1–N3		2.088 (2)
Angles (º)				
O3^{i}–Co1–O4^{i}	57.98 (7)	N1–Co1–O3^{i}		87.17 (8)
O1–Co1–O4^{i}	177.88 (8)	N1–Co1–N5		174.50 (9)
O1–Co1–O3^{i}	120.34 (8)	N5–Co1–O4^{i}		88.06 (9)
O1–Co1–N1	88.10 (9)	N5–Co1–O3^{i}		88.86 (9)
O1–Co1–N5	90.63 (9)	N3–Co1–O4^{i}		89.77 (8)
O1–Co1–N3	91.90 (8)	N3–Co1–O3^{i}		147.75 (8)
N1–Co1–O4^{i}	93.05 (9)	N3–Co1–N1		95.31 (9)
N3–Co1–N5	90.08 (9)			
Hydrogen bond geometry (Å, º)				
D–H···*A*	*D*–H	H···*A*	*D*···*A*	*D*–H···*A*
O7–H7*A*···O4^{iii}	0.85	2.09	2.931(4)	168
O7–H7*B*···O2	0.85	1.91	2.760(3)	176

*Symmetry codes: (i) −x+1/2, y+1/2, −z+3/2; (ii) −x+1/2, y−1/2, −z+3/2, (iii) −x+1, −y, −z+2.

Optical absorption and thermal properties

Solid state UV-Vis diffuse reflectance spectra of the compounds were acquired at room temperature to determine optical absorption properties and evaluate semiconductor properties. Solid state UV-Vis absorption spectra and curves of Kubelka–Munk function of free ligand 5-nipH_2 and the complexes as a function of energy are given in Figure 7. The optical band gap (Eg) was determined by extrapolation from the linear portion of absorption edges based on Kubelka–Munk function (the curve of $(hvF(R))^{1/2}$ versus photon energy (hv): where, hv is the photon energy, F(R) is Kubelka–Munk function ($F(R) = (1–R)^2/2R$). The Eg values of 5-nipH_2 and complexes **1** and **2** are 2.93, 2.85 and 2.874 eV, respectively. These results show the semi-conductive properties of complexes **1** and **2** and complex **1** displays higher conductivity than complex **2**.

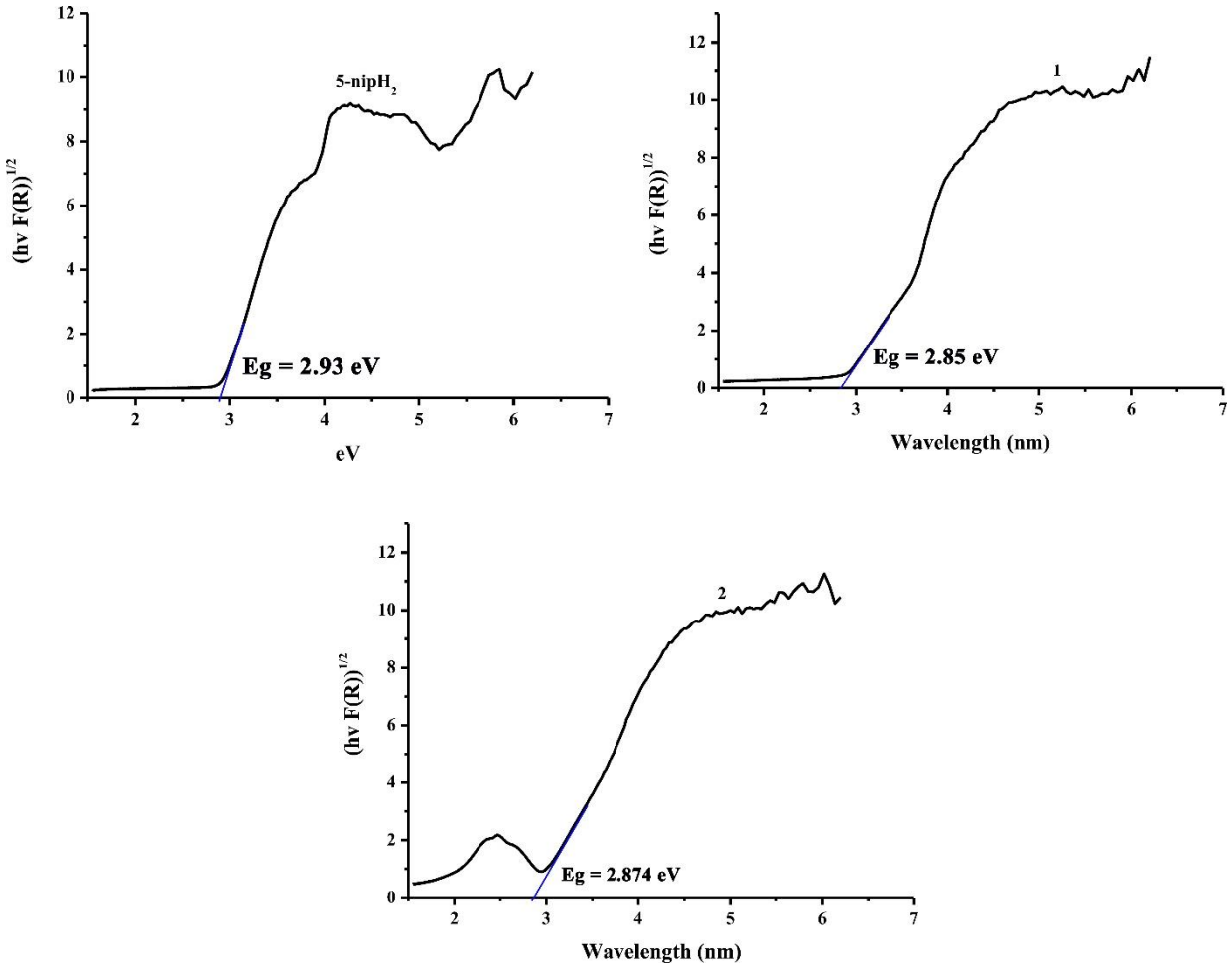

Figure 7: Plots of Kubelka-Munk as a function of energy for free ligand 5-nipH_2 and complexes **1** and **2.**

In order to determine thermal behaviors and stabilities of title complexes, simultaneous TG/DTA analyses were carried out (Figures 8 and 9). For complexes **1** and **2**, the first weight losses in the temperature range 40-125 °C are related to elimination of coordinated and uncoordinated water molecules (found: 4.80 %, calcd.: 4.033 % for **1**; found: 3.50 %, calcd.: 3.40 % for **2**). After these steps, the weight losses of 35.34% in the temperature range 160-368 °C for **1** and 45.5 % in the temperature range 118-365 °C for **2** correspond to the removal of 1-meim ligands. On further heating, the complexes were completely decomposed with exothermic picks and remaining products are possibly MnO and CoO (found: 15.62 %, calcd.: 15.90 % for **1**; found: 14.13 %, calcd.: 14.08 % for **2**).

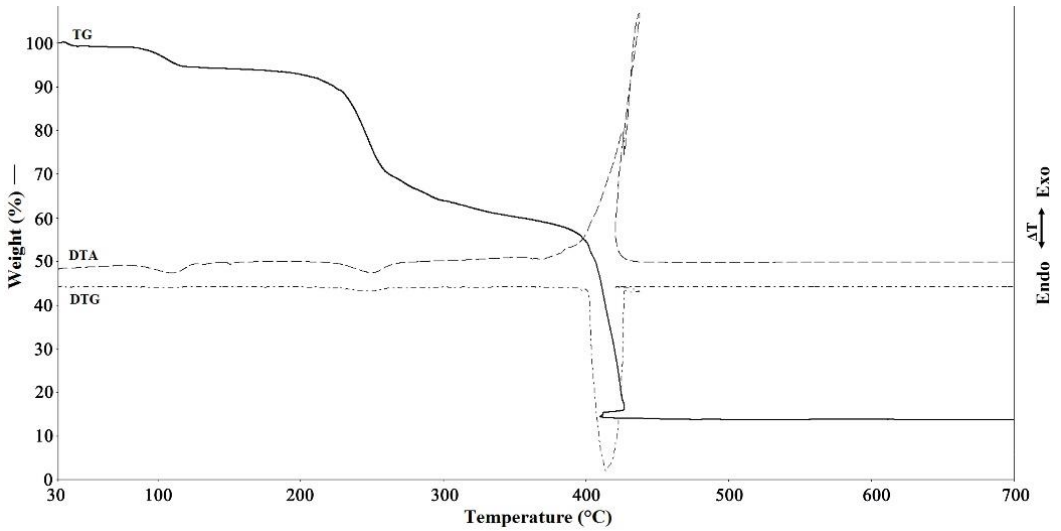

Figure 8: TG, DTG, and DTA curves of complex **1.**

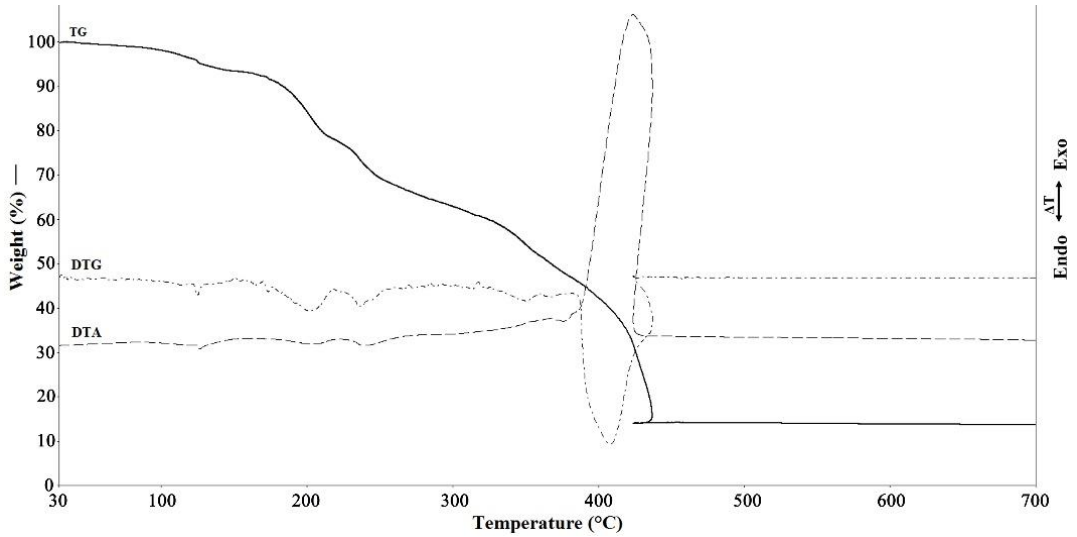

Figure 9: TG, DTG and DTA curves of complex **2.**

CONCLUSION

In this study, two new Mn(II) and Co(II)-coordination polymers were synthesized and characterized. 5-nip ligand displayed different coordination modes in two structures. 5-nip ligand acted as a bridging ligand between metal(II) centers to form 1D. 2D and 3D supramolecular structures are generated through hydrogen bondings and π···π stacking interactions. Optical band gap results of the complexes showed that complex **1** had higher conductivity than free ligand 5-nipH_2 and complex **2**.

REFERENCES

1. He Y, Zhou W, Qian G, Chen B. Methane storage in metal–organic frameworks. Chemical Society Reviews. 2014;43(16):5657-78.

2. Noro S-i, Ochi R, Inubushi Y, Kubo K, Nakamura T. CH4/CO2 and CH4/C2H6 gas separation using a flexible one-dimensional copper (II) porous coordination polymer. Microporous and Mesoporous Materials. 2015;216:92-6.

3. Gu J-Z, Liang X-X, Cui Y-H, Wu J, Shi Z-F, Kirillov AM. Introducing 2-(2-carboxyphenoxy) terephthalic acid as a new versatile building block for design of diverse coordination polymers: synthesis, structural features, luminescence sensing, and magnetism. CrystEngComm. 2017;19(18):2570-88.

4. Arici M, Yeşilel OZ, Taş M, Demiral H. CO2 and iodine uptake properties of Co (II)-coordination polymer constructed from tetracarboxylic acid and flexible bis (imidazole) linker. Crystal Growth & Design. 2017;17(5):2654-9.

5. Arıcı M, Yeşilel OZ, Büyükgüngör O. Four coordination polymers based on 5-tert-butyl isophthalic acid and rigid bis (imidazol-1yl) benzene linkers: Synthesis, luminescence detection of acetone and optical properties. Journal of Solid State Chemistry. 2017;249:141-8.

6. Wezendonk TA, Santos VP, Nasalevich MA, Warringa QS, Dugulan AI, Chojecki A, et al. Elucidating the Nature of Fe Species during Pyrolysis of the Fe-BTC MOF into Highly Active and Stable Fischer–Tropsch Catalysts. ACS Catalysis. 2016;6(5):3236-47.

7. Zhu X, Sun P-P, Ding J-G, Li B-L, Li H-Y. Tuning cobalt coordination architectures by bis (1, 2, 4-triazol-1-ylmethyl) benzene position isomers and 5-nitroisophthalate. Crystal Growth & Design. 2012;12(8):3992-7.

8. Guo F, Zhu B, Xu G, Zhang M, Zhang X, Zhang J. Tuning structural topologies of five photoluminescent Cd (II) coordination polymers through modifying the substitute group of organic ligand. Journal of Solid State Chemistry. 2013;199:42-8.

9. Zhao F-H, Che Y-X, Zheng J-M. Syntheses, structures and magnetic properties of two new complexes constructed from mixed rigid ligands. Inorganic Chemistry Communications. 2012;16:55-60.

10. Lin J-D, Lin M-Z, Tian C-B, Lin P, Du S-W. Syntheses, topological structures and physical properties of two 2D lanthanide–organic frameworks constructed from 5-nitroisophthalic acid. Journal of Molecular Structure. 2009;938(1):111-6.

11. Huang Y, Yan B, Shao M. Synthesis, crystal structure and photoluminescent properties of four lanthanide 5-nitroisophthalate coordination polymers. Journal of solid state chemistry. 2009;182(4):657-68.

12. Ye J, Wang J, Wu Y, Ye L, Zhang P. Supramolecular coordination networks constructed from infinite one-dimensional chains with 5-nitroisophthalate as bridge. Journal of Molecular Structure. 2008;873(1):35-40.

13. Wang X-L, Xia Z-Q, Wei W, Xie G, Chen S-P, Gao S-L. Synthesis, structure, and thermodynamics of a lanthanide coordination compound incorporating 5-nitroisophthalic acid. The Journal of Chemical Thermodynamics. 2012;55:124-9.

14. Chen Q, Zhu X, Ding J-G, Li B-L, Li H-Y. Syntheses, structures and properties of three cobalt coordination polymers based on flexible bis (triazole) and 5-nitroisophthalate coligands. Journal of Molecular Structure. 2013;1038:194-9.

15. Semerci F. Syntheses and photoluminescence properties of new Zn (II) and Cd (II) coordination polymers prepared from 5-sulfoisophthalate ligand. Turkish Journal of Chemistry. 2017;41(2):243-55.

16. López R, Gómez R. Band-gap energy estimation from diffuse reflectance measurements on sol–gel and commercial TiO2: a comparative study. Journal of Sol-Gel Science and Technology. 2012;61(1):1-7.

17. Dolomanov OV, Bourhis LJ, Gildea RJ, Howard JA, Puschmann H. OLEX2: a complete structure solution, refinement and analysis program. Journal of Applied Crystallography. 2009;42(2):339-41.

18. Macrae CF, Edgington PR, McCabe P, Pidcock E, Shields GP, Taylor R, et al. Mercury: visualization and analysis of crystal structures. Journal of Applied Crystallography. 2006;39(3):453-7.